Sc_6MTe_2 (M = Mn, Fe, Co, Ni): Members of the Flexible Zr_6CoAl_2-Type Family of Compounds

Paul A. Maggard and John D. Corbett*

Department of Chemistry, Iowa State University, Ames, Iowa 50011

Received March 28, 2000

The compounds Sc_6MTe_2 (M = Mn, Fe, Co, Ni) have been prepared by high-temperature solid-state techniques and their structures determined to be hexagonal $P\bar{6}2m$ (No. 189), $Z = 1$, $a = 7.662(1)$ Å, 7.6795(2) Å, 7.6977(4) Å, 7.7235(4) Å and $c = 3.9041(9)$ Å, 3.8368(2) Å, 3.7855(3) Å, 3.7656(3) Å for M = Mn, Fe, Co, and Ni, respectively. Crystal structures were refined for M = Fe and Ni, while M = Mn and Co were assigned as isostructural on the basis of powder diffraction data. The Sc_6MTe_2 compounds belong to a large family with the Zr_6CoAl_2-type structure, an ordered variant of the Fe_2P structure. The structure contains confacial tricapped trigonal prisms of scandium centered alternately by the late transition metal or tellurium atoms. The Sc_6MTe_2 compounds are the electron-poorest examples of this structure type. Extended Hückel band calculations for M = Fe and Ni show that both compounds exhibit largely 1D metal−metal bonding and are predicted to be metallic.

Introduction

The study of metal−metal bonding in solid-state compounds has been facilitated by the discovery of many new phases of the group 3 transition metal chalcogenides. These include Sc_2Te,[1] $(Sc,Y)_8Te_3$,[2] and Sc_9Te_2.[3] The chemistry and metal−metal bonding can be further enriched and enlarged by the addition of late transition metals that stabilize new metal frameworks. Thus, inclusion of these additional metal atoms in $Sc_5Ni_2Te_2$[4] and $Y_5M_2Te_2$ (M = Fe, Co, Ni)[5] have provided further insights into the factors that influence metal-bonded structures. Interestingly, $Sc_5Ni_2Te_2$, with double 1D metal chains, and $Y_5Ni_2Te_2$, with 2D metal layers, may both be shown to arise from condensation of the Gd_3I_3Mn structure,[6] which contains double metal chains built of octahedra.

A growing list of compounds are known to crystallize in the ordered variant of the Fe_2P structure type known as the Zr_6CoAl_2 type.[7,8] In this instance, the unit cell of Fe_2P is tripled, with the early transition metal on the iron positions and the late transition metal and main-group element ordered between the two independent phosphorus sites. Recent examples of this type include Zr_6MTe_2 (M = Mn, Fe, Co, Ni, Ru, Pt),[9] Hf_6MSb_2 (M = Fe, Co, Ni),[10] Zr_6CoAs_2,[11] Dy_6MTe_2 (M = Fe, Co, Ni),[12] and R_6CoTe_2 (R = Y, La).[12] Crystallization of these phases in the Zr_6CoAl_2 structure type has been attributed to the size mismatch between the late transition metals and main-group elements.[9] A similar analogy was found between the $Sc_5Ni_2Te_2$[4] and $Hf_5Co_{1+x}P_{3-x}$[13] compounds, with the former an ordered variant of the latter. Concomitant with this ordering is a decrease in the metal-framework dimensionality from 3D to 1D. Described in this paper is a series of new Sc_6MTe_2 (M = Mn, Fe, Co, Ni) compounds which represent the electron-poorest Zr_6CoAl_2 types that have been reported.

Experimental Section

Syntheses. The synthetic methods for the Sc_6MTe_2 phases were parallel to those that have been described elsewhere.[4] The elements were used as received: Sc turnings, Aldrich 99.7%; Te powder, Aldrich 99.99%; Ni powder, Alfa 99.95%. Preparation of the Sc_2Te_3 precursor has been described previously.[4] An appropriate mixture of Sc_2Te_3, Sc, and Mn, Fe, Co or Ni was pelletized, wrapped in molybdenum foil, and loaded into tantalum tubing inside a He-filled glovebox. (At high temperatures, the late transition metals in contact with the tantalum appear to dissolve, but this occurs to a much smaller extent when the container wall is protected by molybdenum foil.) The tantalum tubing was then arc-welded shut under argon and further sealed inside evacuated fused-silica tubing. Heating between 950 and 1025 °C for 72−168 h and slow cooling (5 °C/h) provided ≥90% yields of the four compounds according to relative intensities of the Guinier powder diffraction components. The observed impurities were ScTe and, at lower yields, unreacted pieces of scandium metal (visual identification), and the appropriate late transition metal. The black compounds are modestly stable in air at room temperature.

Powder X-ray Diffraction. The powder diffraction patterns of Sc_6MTe_2 samples were obtained with the aid of an Enraf-Nonius Guinier powder camera and monochromatic Cu $K\alpha_1$ radiation. The powdered samples were mixed with standard silicon (NIST) and placed between two strips of cellophane tape on a frame that mounted on the sample rotation motor. Lattice parameters (Table 1) were obtained with the aid of least-squares refinement of the indexed lines with the 2θ values calibrated by a nonlinear fit to the positions of the standard silicon lines, and these more precise values were used in the calculation of all distances from structural data.

Single-Crystal Diffraction. Several irregularly shaped, silvery crystals were mounted inside 0.3-mm i.d. glass capillaries and then were sealed off and mounted on metal pins. The crystal qualities were

(1) Maggard, P. A.; Corbett, J. D. *Angew. Chem., Int. Ed. Engl.* **1997**, *18*, 3336.
(2) Maggard, P. A.; Corbett, J. D. *Inorg. Chem.* **1998**, *37*, 814.
(3) Maggard, P. A.; Corbett, J. D. *J. Am. Chem. Soc.* **2000**, *122*, 838.
(4) Maggard, P. A.; Corbett, J. D. *Inorg. Chem.* **1999**, *38*, 1945.
(5) Maggard, P. A.; Corbett, J. D. Manuscript in preparation.
(6) Ebihara, M.; Martin, J. D.; Corbett, J. D. *Inorg. Chem.* **1994**, *33*, 2078.
(7) Kwon, Y.-U.; Sevov, S. C.; Corbett, J. D. *Chem. Mater.* **1990**, *2*, 550.
(8) Villars, P.; Calvert, L. D. *Pearson's Handbook of Crystallographic Data for Intermetallic Phases*, 3rd ed.; American Society for Metals: Materials Park, OH, 1985; Vol. 1.
(9) Wang, C.; Hughbanks, T. *Inorg. Chem.* **1996**, *35*, 6987.
(10) Kleinke, H. *J. Alloys Compd.* **1998**, *270*, 136.
(11) Kleinke, H. *J. Alloys Compd.* **1997**, *252*, L29.
(12) Bestaoui, N.; Herle, P. S.; Corbett, J. D. *J. Solid State Chem.*, accepted.
(13) (a) Kleinke, H.; Franzen, H. F. *J. Alloys Compd.* **1996**, *238*, 68. (b) Kleinke, H.; Franzen, H. F. *J. Alloys Compd.* **1997**, *255*, 110.

10.1021/ic0003269 CCC: $19.00
Published on Web 08/17/2000

Table 1. Lattice Constants (Å) and Cell Volumes (Å^3) for Sc_6MTe_2 (M = Mn, Fe, Co, Ni)

compd[a]	*a*	*c*	*V*
Sc_6MnTe_2	7.662(1)	3.9041(9)	198.51(8)
Sc_6FeTe_2	7.6795(2)	3.8368(2)	195.96(2)
Sc_6CoTe_2	7.6977(4)	3.7855(3)	194.26(3)
Sc_6NiTe_2	7.7235(4)	3.7656(3)	194.53(2)

[a] Guinier data, Cu Kα_1, 23 °C, with 11, 15, 18, and 17 indexed lines for Mn, Fe, Co, and Ni, respectively.

Table 2. Some Data Collection and Refinement Parameters for Sc_6MTe_2, M = Fe (First Value) and Ni (Second Value)[a]

fw	580.81, 583.67
space group, *Z*	$P\bar{6}2m$ (No. 189), 1
d_{calc}, g/cm^3	4.921, 4.982
μ, cm^{-1} (Mo Kα_1)	139.29, 145.99
R/R_w[b] (%)	3.8/3.3, 3.1/4.0

[a] Lattice parameters are in Table 1. [b] $R = \sum||F_o| - |F_c||/\sum|F_o|$; $R_w = [\sum w(|F_o| - |F_c|)^2/\sum w(F_o)^2]^{1/2}$, $w = 1/\sigma^2$.

Table 3. Positional and Isotropic-Equivalent Thermal Parameters for Sc_6MTe_2, M = Fe and Ni, Respectively

atom	*x*	*y*	*z*	B_{eq} (Å^2)[a]
Sc1	0.2369(2)	0	$^1/_2$	0.77(6)
	0.2393(3)			0.8(1)
Sc2	0.6117(3)	0	0	0.80(6)
	0.6075(4)			0.7(1)
M	0	0	0	1.24(4)
				1.27(7)
Te	$^1/_3$	$^2/_3$	$^1/_2$	0.62(2)
				0.61(3)

[a] $B_{eq} = \Sigma_i\Sigma_j \mathbf{U}_{ij} a_i^* a_j^* \vec{a}_i \vec{a}_j$.

checked by means of Laue photographs. Diffraction data sets for the best crystals from reactions loaded as Sc_6FeTe_2 and Sc_6NiTe_2 were measured at room temperature on Rigaku AFC6R and CAD4 diffractometers (with monochromated Mo Kα_1 radiation), respectively. Twenty-five centered reflections gathered from a random search were used to determine provisional lattice constants and the probable crystal systems. The data were corrected for Lorentz and polarization effects, and were further corrected for absorption with the aid of three and two ψ-scans, respectively. From totals of 1258 (Fe) and 902 (Ni) reflections measured to $2\theta_{max} = 60°$ and 54°, 1225 and 863 had $I > 3\sigma_I$, and 253 and 239 of these were unique, respectively. Extinction conditions and statistical evidence for noncentricity indicated four possible space groups. Attempts to solve the structures by direct methods (SHELXS[14]) and to refine these with the package TEXSAN[15] were successful only in space group $P\bar{6}2m$ (No. 189). The data averaged with $R_{av} = 6.4$ and 5.5% for $I > 0$. The final anisotropic refinements were $R(F)/R_w = 3.8/3.3$ and 3.1/4.0% for the compositions Sc_6FeTe_2 and Sc_6NiTe_2. Some refinement data for these studies are listed in Table 2, and the atomic positions and isotropic-equivalent temperature factors are given in Table 3. Additional data collection and refinement parameters, the anisotropic displacement parameters, and the complete distance tabulations are in the Supporting Information. These as well as the F_o/F_c listing are also available from J.D.C.

Band Calculations. Extended Hückel calculations were carried out within the tight-binding approximation[16] for the complete structures of Sc_6FeTe_2 and Sc_6NiTe_2 at 140 k-points spread over the irreducible wedge. In order to make the results more appropriate to the charge distributions in these unconventional compounds, H_{ii} parameters employed were those obtained by iteration to charge consistency for Sc and Te in Sc_2Te,[1] and for Fe and Ni in Sc_6FeTe_2 and Sc_6NiTe_2 (this work). These were as follows (in eV): Sc 4s, −6.75; 4p, −3.38; 3d, −6.12; Fe 4s, −5.50; 4p, −2.45; 3d, −6.86; Ni 4s, −5.58; 4p, −2.41; 3d, −7.82; Te 6s, −21.20; 6p, −12.00. The standard orbital exponents were taken from Alvarez.[17]

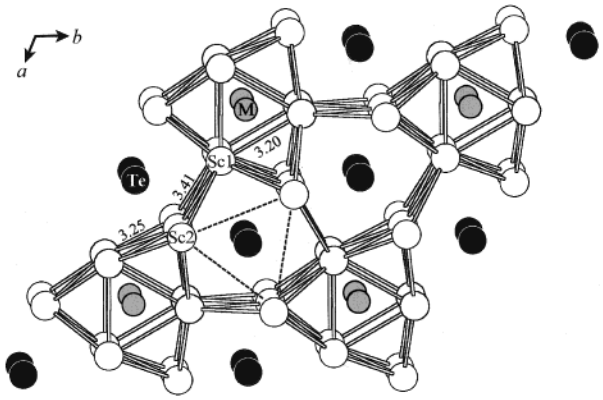

Figure 1. Near-[001] view of the Sc_6MTe_2 structure with M as gray and Te as black circles. Sc−Sc distances (Å) are marked for M = Ni. The dashed lines highlight the trigonal prismatic figures that also surround tellurium. The symmetries at M and Te are $\bar{6}2m$ and $\bar{6}$.

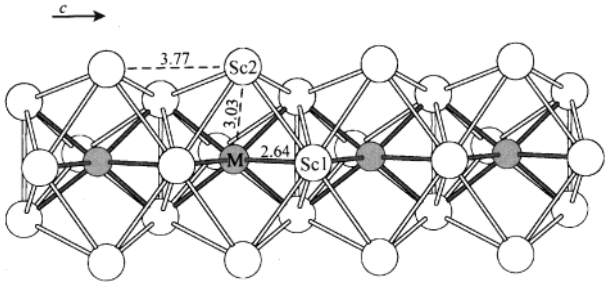

Figure 2. Side view of the isolated Sc_6M metal chain (Figure 1). Sc−M and repeat distances (Å) are for the nickel compound. The dark Sc−M bonds emphasize the Sc1 trigonal prismatic environment around M, which is tricapped by Sc2.

Results and Discussion

Structural Description. The structure along (001) is illustrated in Figure 1 for Sc_6NiTe_2, with selected Sc−Sc distances marked. The late transition metals Mn−Ni center the tricapped trigonal prisms (or tetrakaidecahedra) of scandium that stack and share faces along the *c* axis to form linear chains. The tricapped trigonal prismatic chains are interconnected via Sc1−Sc2 bonds at 3.460(2) and 3.411(3) Å for M = Fe and Ni, respectively. The shorter Sc−Sc distances are around the triangular faces of the trigonal prisms, Sc1−Sc1, 3.151(3) and 3.201(5) Å, and also on the capped rectangular faces, Sc1−Sc2, 3.234(1) and 3.248(2) Å for M = Fe and Ni as before. The next shortest scandium distances in the structure are along the *c* axis for both Sc1−Sc1 and Sc2−Sc2, 3.8368(2) Å (Fe) and 3.7656(3) Å (Ni). Generally, the *c* axes and interchain distances contract between Fe and Ni, while the triangular faces and capping distances around the scandium trigonal prisms (Sc1−Sc2) expand.

A single Sc_6M trigonal prismatic chain is shown in Figure 2 with the axial repeat and Sc−M distances marked for nickel. The dark bonds emphasize the scandium trigonal-prismatic environment around the late transition metal, with Sc1−M lengths of 2.644(1) and 2.638(2) Å, for M = Fe and Ni respectively, while the capping atoms distances, Sc2−M, are 2.982(2) and 3.032(3) Å.

(14) Sheldrick, M. *SHELXS-86*; Universität Göttingen: Germany, 1986.
(15) *TEXSAN*, version 6.0; Molecular Structure Corp.: The Woodlands, TX, 1990.
(16) (a) Hoffman, R. *J. Chem. Phys.* **1963**, *39*, 1397. (b) Whangbo, M.; Hoffman, R. *J. Am. Chem. Soc.* **1978**, *100*, 6093.
(17) Tables of Parameters for Extended Hückel Calculations, Parts 1 and 2, Alvarez, A., University of Barcelona, Barcelona, Spain, 1987.

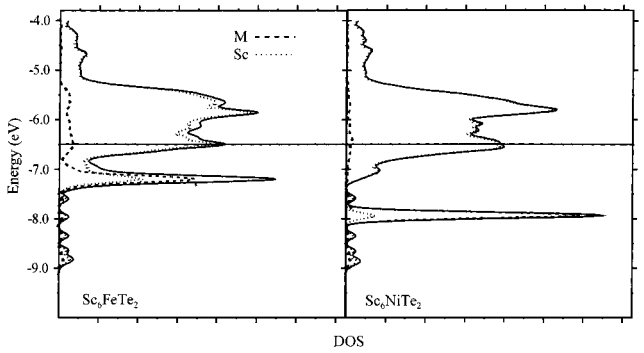

Figure 3. Densities of states from the EHTB band calculations for Sc_6MTe_2, M = Fe, Ni. The separate M (heavier dashed lines) and Sc contributions are projected out. The solid line represents E_F.

The tricapped trigonal prisms about the tellurium atoms, highlighted with dashed lines in Figure 1, are arranged and stacked in an analogous fashion as around the late transition metal, but with some expansion. Six of the Te-centered chains surround each $Sc_{6/2}M$ chain with internal Sc2−Te bonds of 3.0547(6) and 3.0340(8) Å, while distances to the face-capping Sc1 are 3.000(1) and 3.004(2) Å for M = Fe and Ni, respectively. The bonds about Te are generally longer than about M, as might be expected from their size differences, but the distance proportions of the polyhedron about Te are distinctly different from those around M, the capping Sc atoms in the latter being over 0.35 Å more distant than the prismatic members. This contrast does not exist in Zr_6FeTe_2.[9]

Calculations. The Zr_6CoAl_2-type compounds containing scandium are the electron-poorest known in this group, while Zr_6MTe_2 (M = Mn, Fe, Co, Ni, Ru, Pt),[9] Hf_6MSb_2 (M = Fe, Co, Ni),[10] and Zr_6CoAs_2[11] all contain electron-richer transition metals, and with metal−metal bonding arrays that have been described as fully three-dimensional. As just noted, the interchain separations in the present compounds are notably larger. Similar comparisons of other scandium systems such as $(Sc,Y)_8Te_3$[2] and $Sc_5Ni_2Te_2$[4] with electron-richer analogues also show that the lowered electron concentrations in the former lead to both overall weakening of metal−metal interactions and lower dimensionality. Electronic band calculations were employed to understand this aspect in the Sc_6MTe_2 phases better.

Figure 3 shows the total DOS for Sc_6FeTe_2 and Sc_6NiTe_2 with the transition metal contributions projected out for each. The Fermi level (−6.49 eV for both) falls within a large conduction band composed primarily of scandium d states intermixed with some late transition metal d character. Iron d orbitals are higher in energy (about −7.2 eV) and mix more with the scandium d states than do those for nickel (about −8.0 eV). This results in a larger contribution of the iron d states at E_F.

The COOP (crystal orbital overlap population) curves for the total Sc−M and Sc−Sc bonding interactions for each system are plotted in Figure 4. (The M−M interactions are very small.) In both cases, the Sc−M interactions appear to be optimized inasmuch as the Fermi level lies close to the crossover between bonding and antibonding contributions. The host−interstitial bonding is likewise optimized for the systems Zr_6MTe_2 (M = Mn, Fe, Co, Ni, Ru, Pt)[9] and Zr_6CoAs_2.[11] On the other hand, the Sc−Sc COOP data show that many bonding states remain above the Fermi level.

Comparisons of bond distances with overlap populations allow one to ascertain where matrix effects may be important in determining distances, as opposed to real bonding effects. For this purpose, both distances and the corresponding pairwise

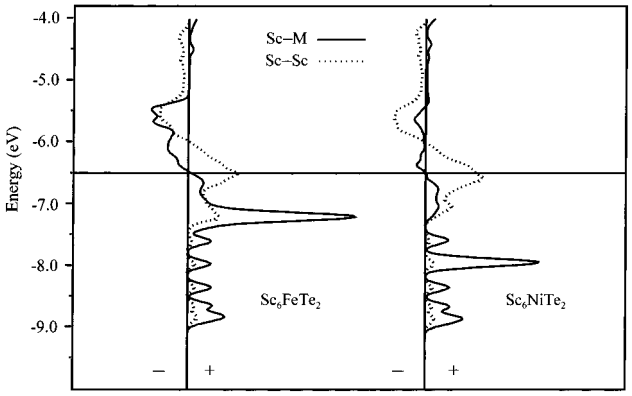

Figure 4. Total COOP (crystal orbital overlap population) curves for indicated pairwise Sc−M (solid line) and Sc−Sc interactions in Sc_6MTe_2.

Table 4. Selected Metal−Metal Distances (Å) and Overlap Populations in Sc_6MTe_2 (M = Fe, Ni)

atom 1	atom 2	distance Fe	distance Ni		overlap population per bond Fe	overlap population per bond Ni
Sc1	Sc1[a]	3.151(3)	3.201(5)	×2	0.228	0.219
Sc1	Sc2	3.234(1)	3.248(2)	×4	0.141	0.146
Sc1	Sc1[b]	3.8368(2)	3.7656(3)	×2	0.048	0.056
Sc1	Sc2[c]	3.460(2)	3.411(3)	×2	0.036	0.041
Sc2	Sc2[b]	3.8368(2)	3.7656(3)	×2	0.002	0.014
Sc1	M	2.644(1)	2.638(2)	×2	0.267	0.189
Sc2	M	2.982(2)	3.032(3)		0.140	0.087
M[b]	M	3.8368(2)	3.7656(3)	×2	−0.008	−0.007

[a] Distance within the triangular faces of the trigonal prism. [b] Distance along *c* axis. [c] Interchain separation.

overlap populations (OP) in Sc_6FeTe_2 and Sc_6NiTe_2 are given for Sc−Sc, Sc−M, and M−M in Table 4, ordered according to the OP values of each type. The largest Sc−Sc OP, and presumably a strong bond, occurs for Sc1−Sc1 on the triangular (end) faces of the trigonal prisms, 0.228 and 0.219 for M = Fe and Ni. The Sc1−Sc2 face caps on the trigonal prism likewise have sizable 0.141 and 0.146 values. Two of the three next largest overlap populations (≤0.056) occur for Sc1−Sc1 and Sc2−Sc2 down the relatively long (∼3.8 Å) *c* axis repeat. The interchain overlap populations for Sc1−Sc2 (0.036−0.041) reflect the reduced dimensionality of the metal−metal bonding in these compounds, being less than one-fifth of the largest internal populations in the chains. However, whether these are particularly unusual is doubtful; as usual, bonds located on the periphery of the metal cluster chains have substantially lower bond populations.[2] The metal−metal bonding is, at the least, located preferentially within the 1D chains of tricapped trigonal prisms, while bond populations fall off regularly with an increased number of tellurium neighbors to the metal atoms involved.

The Sc−M overlap populations show similar trends for M = Fe and Ni. The values for Sc1−M for each contact within the trigonal prisms (0.267, 0.189) are about twice as large as those for the capping Sc2−M populations (0.140, 0.087), in parallel with the distances and always less for nickel. In contrast, M−M interactions between the late transition metal neighbors along the chain are very small and slightly antibonding. The overall trend from the Fe to the Ni compound is that four out of the five Sc−Sc overlap populations increase, while those for both Sc−M bonds decrease. This represents a reapportioning of the metal electrons from the Sc−M framework to the Sc−Sc bonds as the later transition metal d orbitals fall in energy

and take on a more core-like character together with a small compression of the trigonal prism along *c* owing to a decreased interstitial size.

Conclusions. New phases with compositions Sc_6MTe_2 (M = Mn, Fe, Co, Ni) have been synthesized in the Zr_6CoAl_2-type structure. A growing number of examples for this structural type demonstrates its structural and electronic flexibility. Size differences between the later transition metal M and the main-group element Te result in the ordered occupancy of the two different phosphorus sites in the Fe_2P parent structure. The metal−metal bonding characters are more 1D in character than for electron-richer analogues of zirconium etc., while the overlap population trends reflect how the metal-based electrons redistribute from Sc−M to Sc−Sc bonds between Fe and Ni, and probably over the whole series Mn−Ni.

Acknowledgment. We thank R. A. Jacobson for provision of diffractometer time. This research was supported by the National Science Foundation, Solid State Chemistry, via Grants DMR-9510278 and DMR-9809850, and was carried out in the facilities of Ames Laboratory, U.S. Department of Energy.

Supporting Information Available: Tables of additional crystallographic information, anisotropic thermal parameters, and a complete listing of nearest neighbor distances in Sc_6FeTe_2 and Sc_6NiTe_2. This material is available free of charge via the Internet at http://pubs.acs.org.

IC0003269